Eng. Sci., 2025, **38**, 1806

Engineered Science
DOI: https://dx.doi.org/10.30919/es1806

Numerical Modeling of Ultrasound-Induced Tissue Deformation and Thermal Effects for Muscle Pain and Office Syndrome with a Focus on Frequency-Dependent Therapeutic Outcomes

Prempreeya Montienthong,[1,2,*] Nattapon Jaisumroum[1] and Phadungsak Rattanadecho[2,*]

Abstract

This study uses advanced numerical modeling to examine ultrasound waves' effects on muscle tissue and optimize treatment parameters like frequency and exposure length to improve therapeutic efficacy. The COMSOL Multiphysics model accurately simulates tissue mechanical and thermal reactions to ultrasonic stimulation by integrating acoustic wave propagation, viscoelastic tissue deformation, and bioheat transfer equations. Lower ultrasound frequencies (1.0 MHz) induce greater peak mechanical displacement, promoting deeper tissue penetration, while higher frequencies (1.5 MHz) produce a more uniform but reduced deformation gradient, optimizing localized therapeutic effects and minimizing tissue stress. The model confirms a time-dependent dissipation effect in which tissue adapts to prolonged ultrasonic treatment, diminishing mechanical sensitivity. Further, bioheat transfer research shows that ultrasound-induced heating follows Fourier's Law, with energy dissipation mediated by conduction and blood perfusion. This study reduces human and animal experiments by using numerical models to anticipate therapeutic outcomes and ensure patient safety in early treatment planning. The findings demonstrate the therapeutic viability of non-invasive, drug-free ultrasound therapy, eliminating surgical and medication risks. These findings improve muscle pain and office syndrome ultrasound therapy methods, laying the groundwork for individualized and effective treatment.

Keywords: Ultrasound therapy; Office syndrome; Muscle pain; COMSOL Multiphysics; Frequency optimization; Therapeutic heat.

Received: 19 May 2025; Revised: 19 August 2025; Accepted: 16 September 2025.
Article type: Research article.

1. Introduction

Ultrasound technology has been continuously developed since the mid-20th century and has become an essential tool in various medical and scientific fields. Ultrasound refers to sound waves with frequencies above 20 kHz, which exceed the upper limit of human hearing. Due to its ability to penetrate and reflect through different tissues, ultrasound is widely used in diagnosing and treating various medical conditions. Examples include detecting abnormalities in the abdominal cavity, monitoring fetal development, and examining blood vessels in different parts of the body.[1] Beyond diagnostic and therapeutic applications, ultrasound has gained attention in physical therapy, particularly for pain relief, inflammation reduction, and tissue healing. Therapeutic ultrasound offers the advantage of being drug-free and reducing risks associated with surgical interventions. The mechanism involves using sound waves to increase tissue temperature and stimulate blood circulation in the treated area, thereby relaxing muscles and reducing inflammation effectively.[2]

Historically, many researchers have examined the effects of electromagnetic waves, mechanical waves, and ultrasonic waves on various natural phenomena related to agriculture, food, and medicine. The medical applications of ultrasound have been thoroughly examined, especially in diagnostic imaging, physiotherapy, and novel therapeutic techniques, including focused ultrasound for neuromodulation and targeted tumor therapy.[3-7] Moreover, ultrasound-based methodologies have been investigated for wound healing, dermatological treatment, and body sculpting.[8-9]

[1] *Department of Sustainable Development Technology, Faculty of Science and Technology, Thammasat University (Rangsit Campus), Pathumthani 12120, Thailand*
[2] *Hub of Talents Electromagnetic Energy Utilization in Medical Engineering, Department of Mechanical Engineering, Faculty of Engineering, Thammasat University, Khlong Luang, Pathum Thani, 12120, Thailand*
**Email:* ratphadu@engr.tu.ac.th (P. Rattanadecho); prempreeya@tu.ac.th (P. Montienthong)

Computational and experimental models offer insights into the thermal, acoustic, and thermomechanical reactions of biological tissues.[10-19]

Electric field-based technologies, originally designed for industrial and technical purposes, have shown growing promise in biomedical fields, especially in cancer treatment and tissue ablation, via mechanisms like irreversible electroporation.[20] In addition to medicinal and therapeutic applications, ultrasound and electric fields have been utilized to enhance the quality, safety, and energy efficiency of food and agricultural processing systems.[21-24] These works collectively underscore the multifaceted significance of ultrasonic and electric field technology in medical, food engineering, and agricultural processing.

Our research teams have investigated lasers, electromagnetic waves, and mechanical waves in relation to various natural phenomena relevant to natural medicine. Examples of our group's efforts include Bhargava and Rattanadecho examined the application of microwave imaging for breast cancer detection. Their simulation-based analysis evaluated the specific absorption rate (SAR) and temperature distribution in tumors among different age groups and cancer types, highlighting the potential of microwave imaging as a non-invasive diagnostic technique. This study emphasizes the importance of age- and type-specific variables in improving imaging efficacy.[3] Mongkol *et al*. presented a multiphysics simulation model for laser hair removal. Our study integrates light transport, heat transfer, and mechanical deformation to evaluate the photo-thermo-mechanical effects during laser treatment. This study provides insights into the optimization of laser parameters for effective hair removal while minimizing skin damage.[4] Montienthong and Rattanadecho investigated focused ultrasound ablation for the treatment of localized, deformed breast cancer through computational simulations. Our findings underscore the effectiveness of focused ultrasound in achieving targeted ablation while preserving surrounding healthy tissues, thus promoting non-invasive cancer treatments.[5] Wessapan and Rattanadecho examined the effects of acoustic streaming on fluid dynamics and thermal transfer in porous tissues exposed to focused ultrasound. Our research provides essential insights for improving the precision and effectiveness of ultrasound-based therapeutic techniques by analyzing the impact of acoustic streaming on heat and mass transfer mechanisms.[6] Wessapan and Rattanadecho investigated the thermal impacts of metal implants located within various tissue layers subjected to electromagnetic field exposure. Our research highlights the potential risks associated with implant heating and provides guidelines for the safe implementation of electromagnetic-based medical therapies in patients with implants.[7] Wongchadakul P, Rattanadecho P, and Jiamjiroch K. study how heat moves in Low-Level Laser Therapy (LLLT) and how this affects treatment success, pain feeling, and healing of dry skin wounds. The experimental results indicate that the elevation of skin temperature resulting from LLLT directly influences treatment efficacy and pain intensity. Factors that significantly affect the healing process encompass laser power, irradiation frequency, and treatment duration. Research indicates that appropriate temperature regulation can enhance tissue regeneration while minimizing pain levels.[8] P. Wongchadakul and P. Rattanadecho develop a three-dimensional thermomechanical model to simulate laser heating, taking into account the effects of wavelength, laser irradiation intensity, and beam area. The model effectively simulates heat transfer and mechanical alterations in materials subjected to laser irradiation. The findings demonstrate that both wavelength and laser intensity significantly influence heat distribution and mechanical deformation. The beam size has a significant impact on temperature distribution, which is essential for accurate control in industrial and medical applications.[9]

In contemporary settings, conditions like office syndrome and chronic muscle pain constitute major health concerns, particularly for those involved in sedentary occupations. Treatment modalities for these conditions encompass pharmacotherapy, physical rehabilitation, and ultrasound application. Studies indicate that ultrasound therapy can enhance blood flow to muscles and significantly reduce inflammation. However, achieving optimal therapeutic outcomes requires understanding parameters such as frequency, and treatment duration to tailor approaches to individual patients. This research aims to develop ultrasound-based techniques for treating muscle pain and office syndrome through numerical simulations using COMSOL Multiphysics. The study enables detailed analysis of ultrasound effects on muscle tissue at the structural level, including heat distribution. The study focuses on modeling key variables influencing therapy, such as frequency, to identify the most effective methods for alleviating pain and inflammation while minimizing adverse effects.

Recent advancements have occurred in the computational modeling and control of energy-based therapeutic modalities, especially those utilizing focused ultrasound and laser heating mechanisms. The integration of multiphysics simulation platforms, including COMSOL Multiphysics, facilitates precise predictions of tissue responses to thermal and mechanical stimuli, thereby establishing a foundation for personalized, non-invasive treatment protocols. Chaki *et al.* examined the effects of pulsed versus continuous waveforms in high-intensity laser light therapy on deep tissue penetration. The study utilized COMSOL's bioheat transfer models to examine the impact of light fluence and heat propagation on deeper muscle layers. This highlights the increasing importance of precise modeling of bioheat distribution in heterogeneous biological media, such as muscle tissues, which is crucial for developing therapies that reduce discomfort and prevent thermal damage.[25] Dai *et al*. developed a robot-assisted, MRI-guided focused ultrasound therapy platform that employs learning-based algorithms to correct acoustic phase aberration. The integration of COMSOL Multiphysics

with MATLAB simulations facilitated the development of an automated and precise control mechanism for low- and high-intensity focused ultrasound (FUS) treatments. Their findings emphasized the necessity of integrating real-time feedback and anatomical variability into treatment planning, illustrating the evolution of simulation from static models to dynamic, patient-specific solutions.[26] The complexity of temperature evolution in bone and surrounding tissues under high-intensity ultrasound was examined by Ten Eikelder *et al*. who enhanced the Pennes bioheat equation by incorporating shear wave coupling and anisotropic tissue models. Their findings highlighted the necessity of considering both acoustic wave number effects and layered biological structures, especially at muscle-bone interfaces where reflection and scattering are significant.[27] The thermal behavior at the microvascular level has been examined. Paul *et al* performed in vitro experiments and simulations on vascularized tissue phantoms subjected to photothermal therapy. The study employed the Pennes and dual-phase-lag bioheat equations to evaluate transient thermal distributions, highlighting the influence of microstructure, perfusion rate, and nanoparticle enhancement on safety and efficacy.[28] Contemporary studies illustrate the critical importance of numerical simulation in improving precision medicine, especially regarding ultrasound-based therapy for musculoskeletal conditions. The integration of computational frameworks diminishes reliance on empirical and animal models while promoting safer, more effective, and personalized therapeutic results.

This study presents an innovative numerical modeling framework for examining the intricate interactions between ultrasonic waves and muscle tissue, focusing specifically on tissue deformation—an element frequently neglected in prior simulation-based or experimental investigations. This study enhances the understanding of ultrasonic therapy by incorporating biomechanical and thermal processes, surpassing traditional clinical and animal research. The model integrates the Helmholtz Wave Equation for acoustic propagation, Navier's Equation for solid mechanics to represent tissue deformation and stress distribution, and Pennes' Bioheat Transfer Equation to assess heat dissipation in biological tissues.

This research's principal feature is its detailed simulation of tissue deformation in response to different ultrasonic frequencies (1.0 MHz and 1.5 MHz), providing novel insights into displacement fields, mechanical stress patterns, and localized heat effects. This study is differentiated from previous research by the incorporation of mechanical strain factors, which were primarily overlooked in favor of thermal effects. This computational technique reduces the necessity for initial in vivo experiments while delivering high-resolution predictions on treatment efficacy, safety thresholds, and optimum exposure parameters. The findings endorse the creation of tailored ultrasound therapy protocols and highlight the clinical promise of non-invasive, frequency-dependent treatments for muscle pain management, including disorders like office syndrome.

2. Problem formulation

In order to replicate the physical properties of the muscle tissue, such as its density and thermal conductivity, a model of the muscle tissue is constructed in COMSOL Multiphysics by employing the Finite Element Method (FEM). In order to guarantee that the simulation scenarios are as realistic as possible, the parameters of the ultrasound, such as its frequency, are established based on the findings from the literature review. It is possible to conduct an accurate investigation of the effects that ultrasonic waves have on muscle tissue since the model is designed to mirror the therapeutic conditions that are seen in the actual world.

The use of 1.0 MHz and 1.5 MHz ultrasound frequencies in this investigation is based on established clinical standards and previous literature. Therapeutic ultrasound protocols indicate that 1.0 MHz is commonly employed for targeting deep tissues (up to 5 cm), such as the lower back or hip musculature, owing to its reduced attenuation and enhanced penetration capacity.[29,30] Conversely, 1.5 MHz offers more absorption, making it appropriate for the treatment of superficial muscles at depths of 2–3 cm, including regions frequently impacted by office syndrome, such as the neck, shoulders, and upper back.[31,32] These frequencies are not only common in commercial treatment devices but also function as clinical standards for assessing depth-dependent physiological responses. Their selection guarantees that the simulation outcomes are therapeutically pertinent and applicable to actual treatment activities.

2.1 Numerical simulation modeling

The numerical model is developed utilizing physics-based governing equations pertinent to acoustic wave propagation, energy absorption, and heat transfer in biological tissues. The Helmholtz wave governs the acoustic pressure field, characterizing the propagation and interaction of ultrasonic waves in heterogeneous tissue media.[10] The exponential attenuation law characterizes the spatial reduction of wave intensity resulting from medium-dependent losses, illustrating the gradual decay of acoustic energy in relation to propagation distance.[32] The absorbed acoustic energy, the main heat source in tissue, is quantified through the relationship between wave intensity and local power deposition.[31]

The subsequent thermal response is captured using Pennes' bioheat transfer.[33] This equation incorporates conductive heat diffusion, metabolic heat generation, perfusion-induced cooling, and external heat sources like absorbed ultrasonic energy, thus offering a thorough framework for characterizing heat transport in biological tissues. The viscoelastic mechanical response of soft tissues to acoustic excitation is characterized by Navier's equation of motion,[4] which includes both elastic and viscous deformation components. These formulations facilitate the coupled simulation of acoustic propagation, energy absorption, and thermo-

mechanical effects resulting from focused ultrasound exposure.

2.1.1 Pressure acoustics [10]

The propagation of ultrasound waves in biological tissue is governed by the pressure acoustics formulation, represented by the Helmholtz wave Eq. (1):

$$\nabla(\rho\nabla p) + \omega^2/c^2\, \rho p = 0 \tag{1}$$

which describes the spatial distribution of acoustic pressure under harmonic excitation. In this model, p denotes the acoustic pressure (Pa), ρ is the tissue density (kg/m³), $\omega = 2\pi f$ is the angular frequency corresponding to the applied ultrasound frequency, and $c$is the speed of sound in the tissue (m/s).

2.1.2 Acoustic attenuation and power absorption

Ultrasound waves undergo exponential attenuation as they propagate through biological tissue, a phenomenon described by the attenuation Eq. (2):

$$I(x) = I_0 e^{-\alpha x} \tag{2}$$

which quantifies the gradual reduction in acoustic intensity with depth. In this expression, $I(x)$represents the ultrasound intensity at a given position x, I_0 is the initial intensity at the tissue surface, α is the tissue-specific attenuation coefficient that accounts for absorption and scattering losses, and x denotes the propagation distance.

The conversion of acoustic energy into heat within biological tissue is characterized by the power absorption Eq. (3):

$$Q = \alpha I \tag{3}$$

which expresses the rate at which ultrasound energy is absorbed per unit volume. In this relationship, Q denotes the absorbed acoustic power (W/m³), $\alpha$is the energy absorption coefficient of the tissue (Np/m), and I represents the local ultrasound intensity (W/m²).[31]

2.1.3 Bioheat equation

The thermal response of muscle tissue under ultrasound exposure is governed by the Pennes Bioheat Equation, which models the balance of heat generation, conduction, and dissipation within biological media. This relationship is expressed as Eq. (4):[33]

$$\rho C_p \frac{\partial T}{\partial t} = \nabla \cdot (k\nabla T) + Q_{\text{ultrasound}} - Q_{\text{blood perfusion}} + Q_{\text{metabolic}} \tag{4}$$

where ρ denotes tissue density, C_p the specific heat capacity, Tt he local tissue temperature, and k the thermal conductivity. The term $Q_{\text{ultrasound}}$ represents the heat generated from absorbed ultrasonic energy, whereas $Q_{\text{blood perfusion}}$ accounts for heat removed via perfusing blood acting as a convective sink. Additionally, $Q_{\text{metabolic}}$ reflects endogenous metabolic heat production. These concepts encapsulate the interaction between external acoustic heating and inherent physiological processes, enabling quantitative forecasting of spatiotemporal temperature changes during therapeutic ultrasound application.

2.1.4 Tissue deformation (solid mechanics)

The mechanical response of biological tissue subjected to ultrasound loading is modeled using the solid mechanics framework, in which tissue is treated as a viscoelastic continuum governed by Navier's equation of motion[4], expressed as Eq. (5):

$$\rho \frac{\partial^2 u}{\partial t^2} = \nabla \cdot \sigma + F_V \tag{5}$$

In this formulation, u is the displacement vector (m) describing tissue deformation, σ represents the stress tensor (Pa) that characterizes internal mechanical stresses, F_V denotes the acoustic body force per unit volume (N/m³) generated by ultrasound propagation, and ρ is the tissue density (kg/m³). This equation links inertial effects, internal stress redistribution, and ultrasound-induced body forces, enabling quantitative analysis of how soft tissue deforms under transient acoustic radiation forces during therapeutic ultrasound exposure.

2.1.5 Relation to elastic wave equations

The governing equation for tissue deformation can be directly related to the classical elastic wave equation, which describes the propagation of stress waves— including ultrasonic waves—within solid media. When external body forces are absent $(F_V = 0)$ and the material is assumed to be homogeneous, Navier's equation simplifies to the elastic wave[4] form Eq. (6):

$$\rho \frac{\partial^2 u}{\partial t^2} = \nabla \cdot \sigma \tag{6}$$

where σ is the elastic stress tensor. This stress tensor is linked to the strain tensor through Hooke's Law, with the relationship determined by the material's elastic constants. The reduced form highlights that wave propagation in solids arises from the interplay between inertial forces and elastic restoring forces, providing a fundamental basis for understanding how ultrasonic stress waves travel through biological tissue under idealized linear-elastic conditions.

2.2 Physical model

An axisymmetric tissue model was employed to examine the temperature distribution in biological tissue during ultrasonic therapy. Fig. S1 depicts ultrasound therapy utilized for alleviating muscle pain or promoting tissue recovery, especially in patients suffering from repetitive strain injuries or office syndrome. Fig. 1 (a) illustrates an inverted geometry alongside the essential equations utilized to simulate heat transport in biological tissue through a two dimensions (2D) Axially Symmetrical Model Geometry. The model's

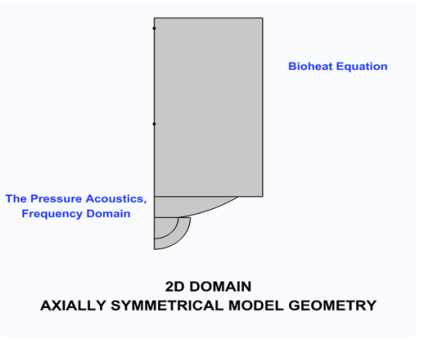

(a)

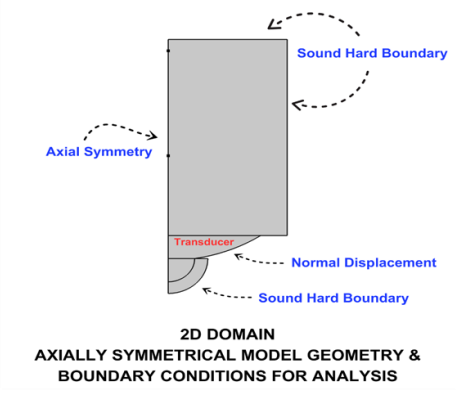

(b)

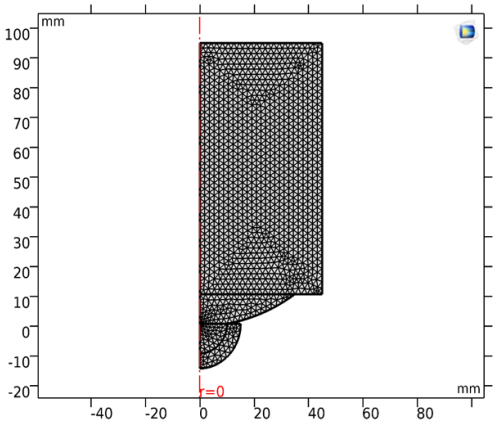

(c)

Fig. 1: The modeling framework used in the study: The inverted geometry domain. The governing equations applied include the bioheat transfer equation application of the Bioheat Transport Equation to examine heat transport within the tissue. $\rho C_p \, \partial T/\partial t = \nabla(k\nabla T) + Q_{ultrasound} - Q_{blood\ prefusion} + Q_{metabolic}$ and the pressure acoustics equation $\nabla(\rho\nabla P) + \frac{\omega^2}{c^2}\rho p = 0$, which are detailed in the main text. (b) The boundary conditions imposed on the inverted geometry model. (c) The meshed geometry illustrating the dimensions and element distribution used in the COMSOL Multiphysics simulation.

Fig. 1(c) illustrates a two-dimensional axisymmetric model employed in the modeling of ultrasonic therapy. The muscle tissue and transducer configuration facilitate ultrasound-induced mechanical displacement, thermal distribution, and therapeutic outcomes. Horizontal Axis, the radial coordinate, referred to as the r-axis, commences at r = 0 mm and extends outward. The highest observable radial extent is roughly 100 mm, equating to a three-dimensional diameter of 200 mm. Vertical Axis, the vertical coordinate, denoted by the z-axis, spans from approximately z ≈ -20 mm to z = 100 mm, resulting in a total model height of around 120 mm. The lower boundary (z ≈ -20 mm) indicates the location of the ultrasound transducer, while the higher limit (z = 100 mm) signifies the interface with the muscular tissue. The muscular tissue area is depicted by the upper rectangular structure, measuring roughly 100 mm in height. The breadth varies from r = 0 mm to approximately 50 mm. This region serves as the primary domain for analyzing ultrasound-induced displacement, heat diffusion, and mechanical effects. The ultrasound transducer, depicted by the lower curved segment, is situated between z = -10 mm and z = 20 mm, with a width ranging from r = 0 mm to about 20 mm, equating to a total three-dimensional measurement of 40 mm. This component generates and transmits ultrasonic waves into the tissue. The axis of symmetry, represented by the vertical red line at r = 0 mm. The chosen measurements precisely depict human muscle tissue exposed to ultrasonic therapy. The 100 mm tissue height guarantees a thorough examination of ultrasonic penetration and thermal diffusion. The 50 mm radial width (equal to 100 mm in full width) corresponds with clinical ultrasonic therapy applications, ensuring applicability to real-world treatments. The ultrasonic transducer width (about 20 mm) aligns with typical medical ultrasound probe dimensions, rendering the model appropriate for mimicking therapeutic ultrasound treatment regimens.

2.2.1 Assumptions and limitations

To simulate the impact of ultrasound on muscle tissue, specifically on temperature elevation and mechanical response, many simplifying assumptions were implemented to improve computational efficiency while maintaining accuracy.

1. A 2D axisymmetric method was employed to simulate muscle tissue shape, thereby decreasing computer complexity while preserving adequate accuracy in assessing tissue function.

2. The simulated muscle tissue was considered homogeneous, exhibiting uniform thermal and mechanical properties, including density, thermal conductivity, and specific heat capacity.

3. The muscle tissue was deemed incompressible, and its mechanical response to ultrasound-induced stress was linear, facilitating the measurement of material deformation.

4. Thermal conductivity and specific heat capacity were presumed to be constant and temperature-independent, hence ensuring computational stability.

5. The absorption of ultrasonic energy adhered to acoustic absorption principles, with the absorbed energy fully transformed into heat, as delineated by Pennes' Bioheat

Transfer Equation.[33]

2.2.2 Initial and boundary conditions

The initial mechanical, acoustic, and thermal fields were assumed to be quiescent prior to ultrasound exposure: $u(x,0)=0$, $\frac{\partial u}{\partial t}(x,0)=0$, $p(x,0)=0$, $T(x,0)=T_0$. Fig. 1(b) illustrates the boundary conditions regulating the interaction among the tissue, transducer, and adjacent media.

2.2.3 Acoustic boundary conditions and ultrasound wave emission (transducer input)

The acoustic excitation applied at the transducer surface is represented by a time-harmonic pressure as described by Eq. (7):

$$p(x,t)=P_0 cos\,(\omega t) \tag{7}$$

where P_0 is the peak pressure, and $\omega=2\pi f$ denotes the angular frequency. The lower boundary of the model functions as a wave receiver, where ultrasound waves are received after they have propagated through the tissue. In order to analyze wave reflections and energy accumulation within the tissue, it is necessary to assume that the walls near the transducer are completely reflecting. This will prevent any absorption of acoustic energy.

2.2.4 Mechanical boundary conditions

Mechanical and thermal boundary conditions were implemented to capture ultrasound–tissue interactions in a physically consistent manner. The transducer–tissue coupling was represented by a prescribed normal displacement $u_n=U_0$, which introduces oscillatory motion into the tissue. Regions attached to rigid anatomical structures were constrained with a fixed boundary condition $u=0$ on Γ_{fixed}, while tissue–air interfaces were assumed to be stress-free, expressed as $\sigma\cdot n=0$, enabling natural deformation under acoustic loading. Ultrasound propagation generates an internal body force described by the acoustic radiation force Eq. (8):

$$F_V=-\frac{\alpha}{\rho c}\nabla(p^2) \tag{8}$$

where α, ρ, and c denote the acoustic attenuation coefficient, tissue density, and sound speed, respectively. Heat transfer at the skin surface was modeled using a convective boundary condition as specified by Eq. (9):

$$-k\nabla T\cdot n=h(T-T_\infty) \tag{9}$$

which k is thermal conductivity, h the convective heat transfer coefficient, and T_∞ the ambient temperature. Blood-mediated thermal dissipation was incorporated through the perfusion heat exchange term, as specified by Eq. (10):

$$Q_{\text{blood}}=\rho_b C_p w_b(T_b-T) \tag{10}$$

where ρ_b, C_p, and w_b correspond to blood density, specific heat capacity, and perfusion rate, and T_b is arterial blood temperature. Collectively, these boundary conditions provide a comprehensive description of mechanical constraints, acoustic forcing, surface cooling, and perfusion-driven heat removal during ultrasound exposure.

The present simulation posits that soft tissues function as homogeneous and linearly elastic materials, thereby streamlining the mechanical model and facilitating computational efficiency. This method aligns with earlier numerical investigations regarding therapeutic ultrasound.[34,35] Biological tissues exhibit inherent heterogeneity, characterized by anisotropic and nonlinear viscoelastic properties, particularly evident in muscle fibers and connective tissues. The assumption of homogeneity may neglect localized thermal gradients and stress concentrations that can occur at tissue interfaces, while linear elasticity may underestimate strain accumulation in tissues exposed to repeated or prolonged sonication. These simplifications, while conventional, may result in slight discrepancies in the prediction of absolute temperature or displacement magnitudes. A sensitivity analysis was performed by varying the Young's modulus and tissue density by ±15 % of their nominal values. The maximum displacement exhibited a variation of less than 4.2 %, while the peak temperature fluctuated by less than 1.9 %, demonstrating the model's robustness amidst moderate parameter variability. Future models may improve anatomical accuracy by integrating multilayer tissue heterogeneity, nonlinear stress-strain relationships, and anisotropic heat diffusion. In clinical practice, these assumptions suggest that the model's predictions should be understood as averaged estimations rather than localized absolute values. Thus, although the current model offers a valid framework for treatment planning and comparative frequency analysis, it is essential to exercise caution when applying the results to individual patient scenarios.

The thermal and acoustic properties incorporated in the simulation encompass key parameters governing heat transfer and ultrasound–tissue interaction. The thermal behavior of the tissue is characterized by the heat transfer coefficient h (W/m²·K), the specific heat capacity c (J/kg·K) describing the energy required to raise tissue temperature, the thermal conductivity k (W/m·K) which dictates heat conduction efficiency, and the density ρ (kg/m³) representing mass per unit volume. Blood-mediated thermal regulation is governed by the perfusion rate ω_b (m³/s·m³), reflecting tissue blood flow and its role in convective heat removal, while metabolic heat generation is represented by Q_{met} (W/m³), accounting for endogenous heat production. The acoustic response of the tissue is determined by the speed of sound c_c (m/s), which defines acoustic propagation velocity, the attenuation coefficient α (dB/cm) that quantifies ultrasound energy loss via absorption and scattering at given frequencies, and the effective viscosity η, which influences the dissipative and mechanical interaction of ultrasound waves with the viscoelastic tissue matrix.

Table 1 indicates that muscle possesses moderate thermal conductivity and density. Elevated sound velocity (1545 ± 5

m/s) and considerable attenuation at elevated frequencies, signifying its efficacy in absorbing ultrasound energy. Blood exhibits a high specific heat capacity and comparatively low attenuation coefficients, indicating its effectiveness in thermal regulation and reduced resistance to ultrasound propagation. These attributes are crucial for the design and optimization of therapeutic interventions, including ultrasound-based diagnostics and treatments.

3. Results and discussion

3.1 Validation of simulation results

To evaluate the accuracy of the existing numerical model, the simulation results were validated and compared to numerical outcomes obtained from geometric models under identical conditions, as shown in Fig. 2. The simulation outcomes were corroborated with previously existing thermal models and experimental datasets often employed for benchmarking heat transfer in ultrasound-exposed tissues.[36-38] This comparison investigation increases trust in the accuracy of the provided numerical model by proving its dependability in simulating heat transfer characteristics in tissues subjected to ultrasonic waves. Nevertheless, disparities may arise because of variations in acoustic and thermal qualities, experimental settings, tissue physical properties, computational methodologies, and the instrumentation used to monitor actual temperature changes.

3.2 Simulation results and discussion

We simulated the effects of ultrasound at a frequency of 1.0 MHz using COMSOL Multiphysics, which included critical modules like Bioheat Transfer and Pressure Acoustics (Frequency Domain). The following was discovered during the simulation that the surface temperature was 36 °C at beginning of the experiment (0 seconds), as determined by the initial conditions. The ultrasound waves targeted the tissue, causing the maximal temperature to increase to 40.09 °C within 20 seconds (Fig. 3b), indicating localized heat accumulation. As heat dissipated into the surrounding areas, the maximum temperature progressively decreased to 36.84 °C between 40 and 100 seconds (Fig. 3f), exhibiting thermal energy transfer through conduction. This heating effect is essential for the relaxation of muscles and the adjacent tissues, the reduction of muscle tension, and the promotion of blood circulation. The results are consistent with the therapeutic applications of ultrasound for the alleviation of muscle pain, particularly in office syndrome patients who

Table 1: The thermal properties and acoustic properties of tissues.[5]

Tissue	h	c	k	ρ	ω_b	Q_{met}	c_c (speed of sound)	α at 1 MHz	α at 1.5 MHz	η
Muscle	15	3800	0.48	1085	5.3908×10^{-4}	700	1545 ± 5	1.09	1.2819	1.4
Blood	—	4200	0.501	1060	—	—	1540	0.1303	0.1532	1.4

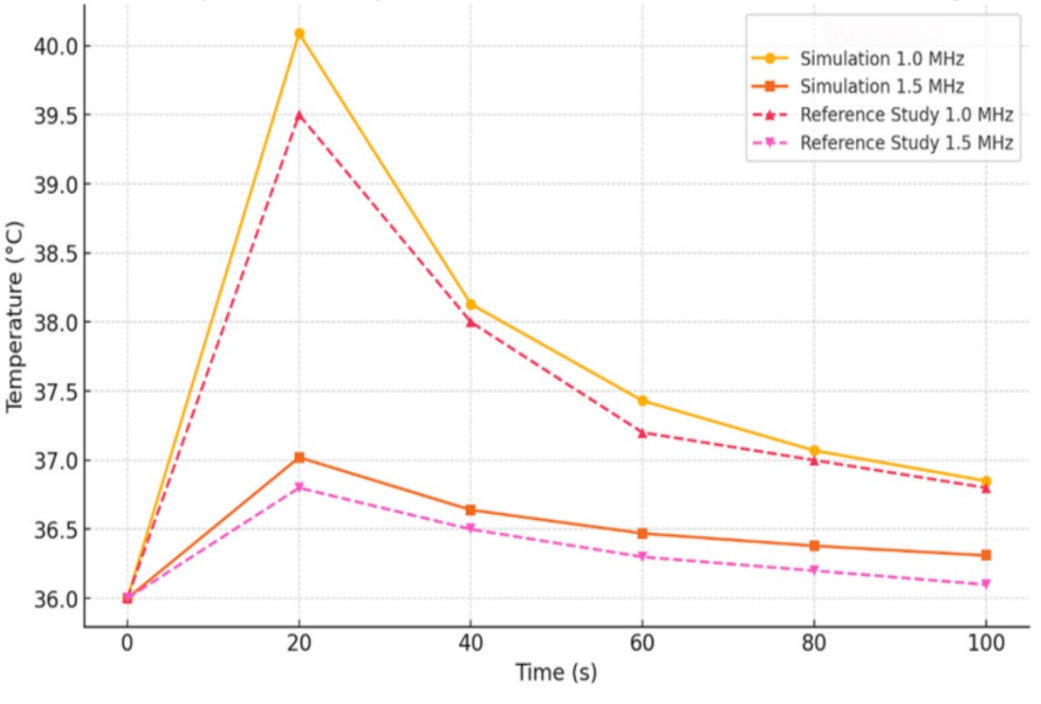

Fig. 2: The validation of the current model by comparing its results with previous studies.[36–38]

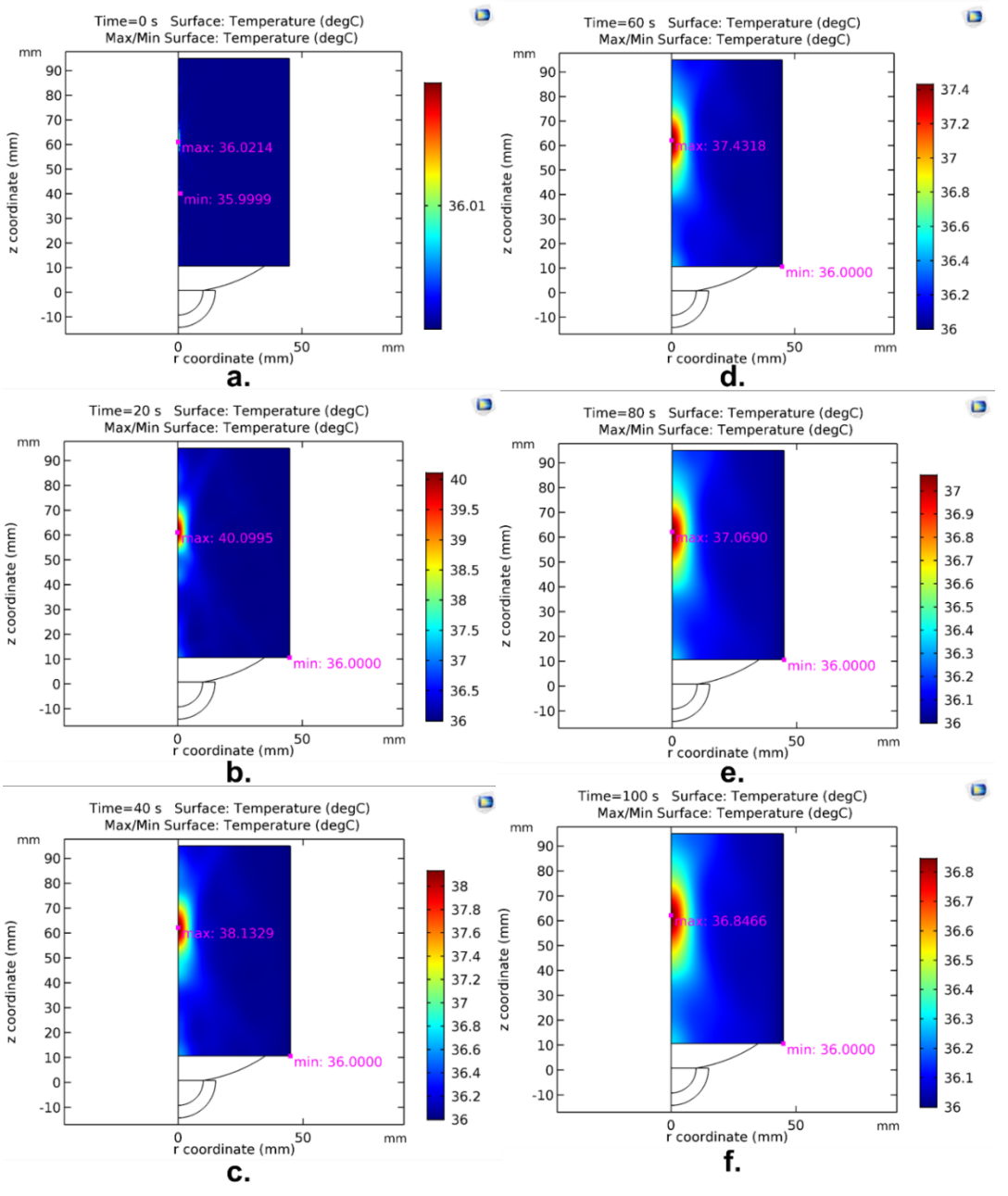

Fig. 3: The temperature distribution (°C) for ultrasound at a frequency of 1.0 MHz at time intervals of (a) 0 s, (b) 20 s, (c) 40 s, (d) 60 s, (e) 80 s, and (f) 100 s.

frequently experience tension in the neck, shoulder, and upper back muscles.

The results also emphasize the therapeutic benefits of ultrasound-induced heating. Ultrasound at 1.0 MHz efficiently produces deep tissue heating, penetrating muscle layers and facilitating muscle relaxation. This alleviates chronic pain, especially in individuals with office syndrome. Robertson *et al.*[39] established that ultrasound waves substantially reduce muscle pain, particularly in individuals with muscle tension or inflammation. The heat produced in the simulation enhances blood circulation in tissues, facilitating the transport of nutrients and oxygen to areas of discomfort. Petersson *et al.*[40] corroborated these findings, demonstrating that ultrasound-induced thermal effects augment microcirculation and diminish the buildup of nociceptive substances like lactic acid.

Ultrasound-induced thermal stimulation diminishes prostaglandin levels and other inflammatory mediators, thereby effectively relieving pain in patients with office syndrome. Ultrasound therapy facilitates the recuperation of injured tissues resulting from repetitive strain, such as extended sitting or static postures in individuals with office syndrome. The simulation underscores the diverse advantages of ultrasound therapy in alleviating chronic muscle pain and promoting tissue recovery, rendering it a promising method for managing office syndrome and associated ailments.

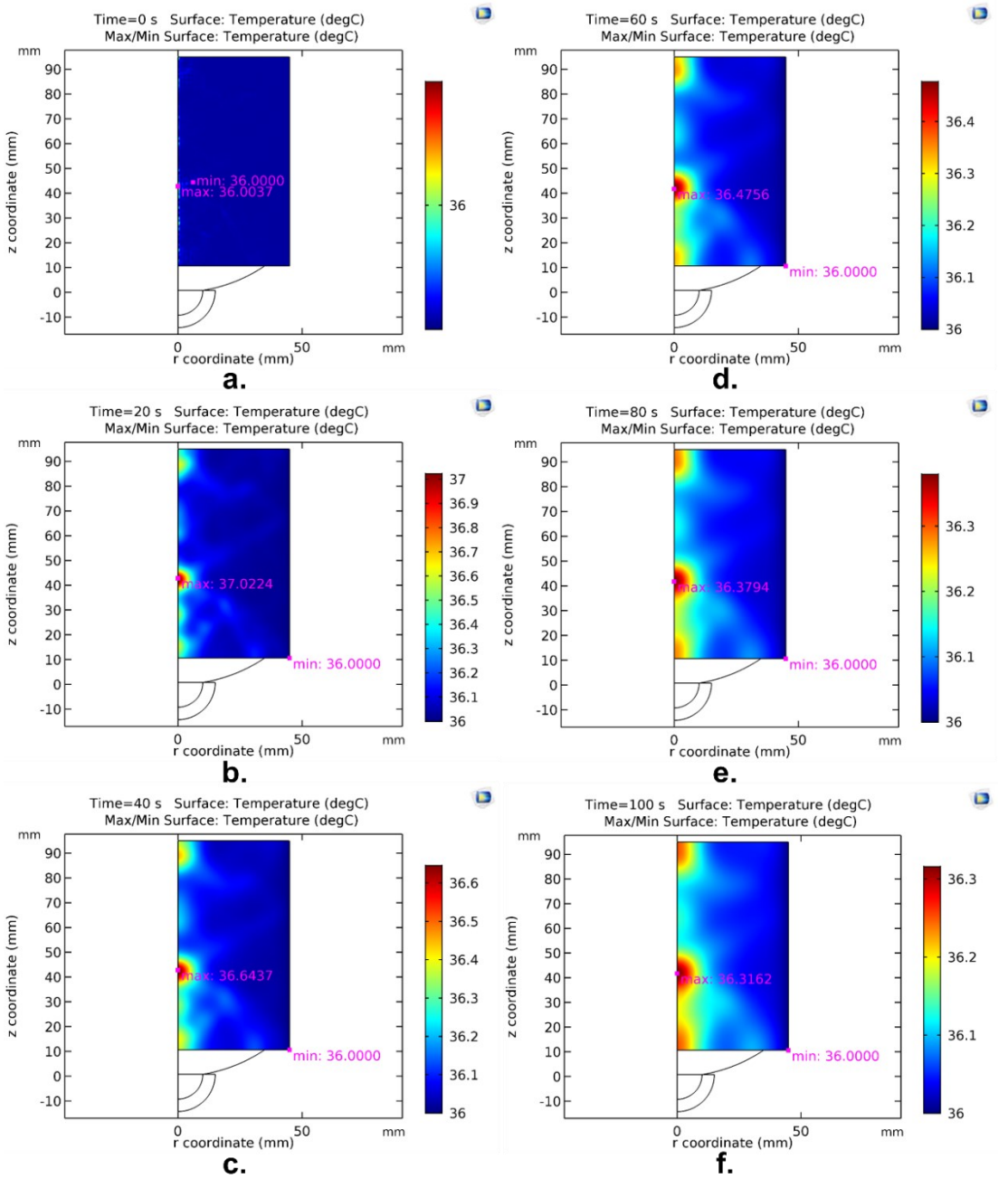

Fig. 4: The temperature distribution (°C) for ultrasound at a frequency of 1.5 MHz at time intervals of (a) 0 s, (b) 20 s, (c) 40 s, (d) 60 s, (e) 80 s, and (f) 100 s.

3.3 Analysis of surface temperature distribution in tissue

The simulation outcomes for ultrasound at 1.5 MHz, illustrated in Fig. 4, exhibit the temperature distribution on the tissue surface across various time intervals from 0 to 100 seconds. The findings demonstrate that the maximum temperature in the simulated area rises over time, beginning from an initial baseline of 36 °C at t = 0 seconds and reaching a peak of 36.3162 °C at t = 100 seconds (Fig. 4f). The increase in temperature indicates the impact of ultrasound-induced heating in the tissue, influenced by its distinct thermal conductivity and acoustic energy absorption characteristics. The maximum temperature is situated close to the ultrasound source, aligning with the principle that acoustic intensity diminishes with distance due to energy absorption in the tissue. The temperature distribution is heterogeneous, exhibiting a decrease in temperature with increasing distance from the ultrasound source. This behavior corresponds with the energy absorption properties outlined by bioheat transfer equations, where in energy absorption decreases as waves propagate. The peak temperature of 36.3162 °C at 1.5 MHz (Fig. 4f) is comfortably below the biological tolerance threshold, as substantial cellular damage generally arises at temperatures surpassing 42 °C. In comparison to the simulation at 1.0 MHz, the thermal accumulation at 1.5 MHz is diminished, with the peak temperature at 1.0 MHz attaining roughly

40 °C. Moreover, energy dissipation at 1.5 MHz transpires more rapidly, indicating variances in energy absorption properties between the two frequencies.

3.4 Comparative analysis of frequency effects

The comparative analysis of temperature distributions at 1.0 MHz (Fig. 3) and 1.5 MHz (Fig. 4) demonstrates distinct thermal behaviors linked to ultrasound frequency. At 1.0 MHz, the maximum temperature increases over time and penetrates more deeply into the tissue, which aligns with the lower absorption and greater penetration depth characteristic of low-frequency ultrasound waves. At 1.5 MHz, the maximum surface temperature increases more rapidly and is highly localized near the transducer due to higher acoustic attenuation, which enhances energy absorption in superficial layers. This phenomenon results in increased heating near the skin surface and diminished heat transfer to deeper tissues. The observed differences can be attributed to three primary factors: (i) acoustic attenuation, which increases with frequency and restricts thermal deposition to superficial tissue at 1.5 MHz; (ii) penetration depth, which is greater at 1.0 MHz facilitating broader heat dispersion into deeper layers; and (iii) energy absorption efficiency, where higher frequencies demonstrate a greater conversion of acoustic energy into heat, thus enhancing localized thermal effects.

The disparities in thermal effects between 1.0 MHz and 1.5 MHz simulations underscore the impact of frequency on ultrasound wave dynamics. Ultrasound waves at 1.5 MHz demonstrate reduced energy penetration relative to 1.0 MHz, in accordance with the principle that higher frequencies are more readily absorbed by superficial tissues.[31] 1.5 MHz ultrasound provides distributed energy appropriate for the treatment of superficial muscles, including those in the neck, shoulders, and upper back. 1.0 MHz Ultrasonography Facilitates enhanced energy penetration, rendering it suitable for addressing deeper musculature, particularly in the lower back or hip areas.[32]

At 1.5 MHz ultrasound. This treatment is suitable for people experiencing superficial pain, like tension in the shoulders, neck, and upper back, which necessitates applying heat to the skin's surface. 1.0 MHz ultrasound frequency. This device is ideal for people who experience chronic pain, like back pain from prolonged sitting. The increase in temperature noted in tissues subjected to ultrasound aligns with theoretical models and prior studies on bioheat transfer.[33] The Pennes Bioheat Equation, utilized in this analysis, has been validated as an effective instrument for numerical simulation in these scenarios, offering a dependable framework for comprehending the thermal effects of ultrasound in therapeutic applications.

Fig. 5 depicts the temperature increase and subsequent stabilization over time, offering a comparative analysis of the thermal effects produced by the two frequencies. Fig. 5 depicts the correlation between time (x-axis) and maximum temperature (y-axis) as modeled for ultrasound frequencies of 1.0 MHz and 1.5 MHz. The graph indicates that at 1.0 MHz, the temperature increase is more significant during the initial phase and diminishes more slowly over 100 seconds, in contrast to 1.5 MHz, where energy dissipates and temperature declines more swiftly. This behavior illustrates the varying energy absorption properties of the two frequencies. At 1.0 MHz, the maximum temperature ascends swiftly from 36.00 °C to 40.09 °C in 20 seconds, subsequently declining to 36.85 °C at 100 seconds. In contrast, at 1.5 MHz, the peak temperature exhibits a minor rise from 36.00 °C to 37.02 °C over 20 seconds, subsequently declining to 36.31 °C at 100 seconds.

The elevated maximum temperature recorded at 1.0 MHz (40.09 °C) relative to 1.5 MHz (37.02 °C) suggests that ultrasound wave energy penetrates more profoundly into the

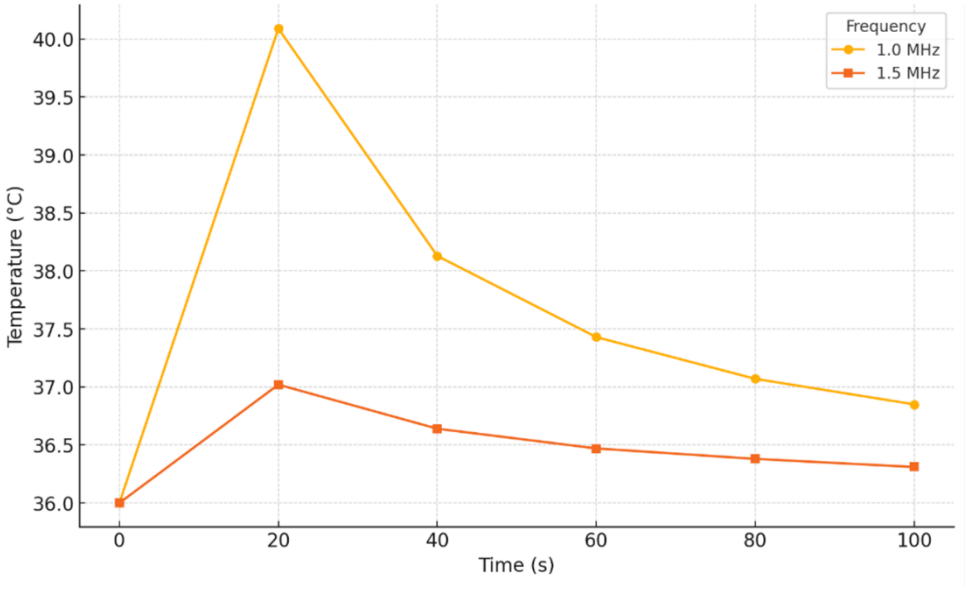

Fig. 5: The relationship between time (x-axis) and maximum temperature (y-axis) as derived from simulations at ultrasound frequencies of 1.0 MHz and 1.5 MHz.

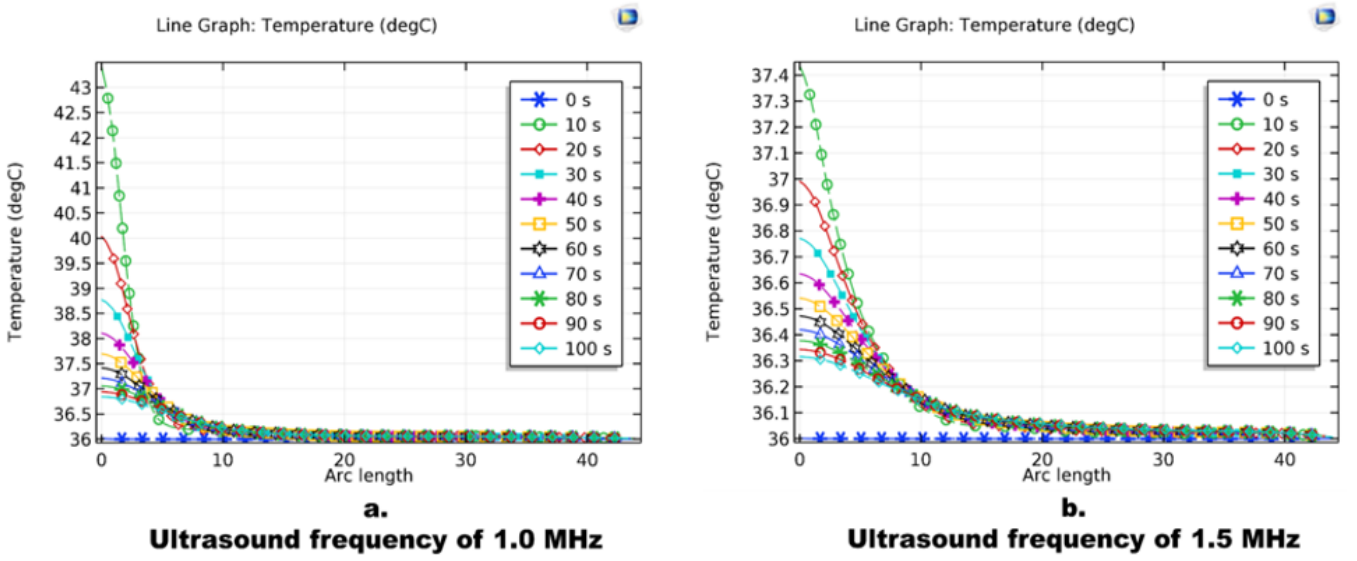

Fig. 6 Temperature distribution along the tissue arc length under ultrasound exposure at two frequencies: (a) 1.0 MHz and (b) 1.5 MHz, evaluated at time intervals from 0 to 100 s.

tissue at lower frequencies. This leads to increased heat retention in deeper tissue strata. Lower frequencies, like 1.0 MHz, facilitate deeper penetration of acoustic energy, rendering them more appropriate for addressing deeper muscle tissues. Conversely, elevated frequencies such as 1.5 MHz demonstrate increased absorption in superficial layers, resulting in expedited energy dissipation and more focused superficial heating effects.

3.5 Effect of temperature distribution

Over time, the thermal energy produced by ultrasound waves dissipates via thermal conduction. At an ultrasound frequency of 1.0 MHz, the temperature progressively declines, signifying continuous heat transfer within deeper tissue strata. Conversely, at 1.5 MHz, the temperature declines more swiftly, indicating energy absorption in superficial tissues and accelerated heat dissipation. This behavior underscores the varying thermal impacts of ultrasound frequencies, with 1.0 MHz being more efficacious for deeper tissue heating, whereas 1.5 MHz facilitates quicker cooling and localized heating in superficial layers.

Fig. S2 illustrates the red cut line in designated regions of the 2D simulation space (ultrasound frequencies of 1.0 MHz and 1.5 MHz), with the temperature distribution along the red cut line represented in a line graph.

Fig. 6a depicts the temperature distribution in muscle tissue, subjecting it to ultrasound waves at frequencies of 1.0 MHz (top graph). The y-axis represents the temperature in degrees Celsius (°C), while the x-axis represents the arc length (distance from the ultrasound source). The results obtained over a range of time intervals (0–100 seconds) emphasize the effects of varying ultrasound frequencies on the distribution of heat and the rise in temperature in tissue. The 1.0 MHz Frequency Graph (Upper Graph), initial temperature as baseline temperature of the tissue, is approximately 36.0 °C prior to ultrasound exposure (0 seconds). Upon application, the temperature near the source rapidly increases. After 10 seconds, the center (arc length = 0) reaches its peak temperature of approximately 43 °C, indicating the characteristics of heat distribution. The temperature diminishes exponentially with increased distance from the source. The heat distribution encompasses a broader arc length than the 1.5 MHz frequency. Temperature diminishes progressively. At 50 and 100 seconds, the temperature near the center diminishes to approximately 37 °C because of heat transfer to adjacent tissues.

Fig. 6b depicts the temperature distribution in muscle tissue, subjecting it to ultrasound waves at frequencies of 1.5 MHz (bottom graph). Initial Temperature is ~36.0 °C. The temperature rise the center region of source (arc length = 0) is slower compared to 1.0 MHz. The maximum temperature (~37.4 °C) occurs near the center (arc length = 0) at 10 seconds. Heat distribution is limited to a shorter arc length (~10 units) near the source. The temperature near the center drops quickly and stabilizes at ~36.3 °C by 100 seconds. The heat dissipation occurs faster due to energy absorption in superficial layers. Therapeutic Implications, the localized heat distribution is ideal for treating superficial muscles, such as those in the neck, shoulders, and upper back, commonly affected by tension or office syndrome. Comparison of 1.0 MHz and 1.5 MHz frequency affects maximum temperature, the 1.0 MHz frequency produces a higher maximum temperature (~40 °C) compared to the 1.5 MHz frequency (~37 °C). Heat Distribution, the 1.0 MHz frequency achieves deeper and wider heat penetration. The 1.5 MHz frequency focuses heat on superficial layers and dissipates energy quickly.

Lower-frequency ultrasound waves, which penetrate deeper and accumulate energy more efficiently, cause this disparity, while superficial tissue layers more readily absorb higher frequencies.[31] The 1.0 MHz frequency exhibited wider

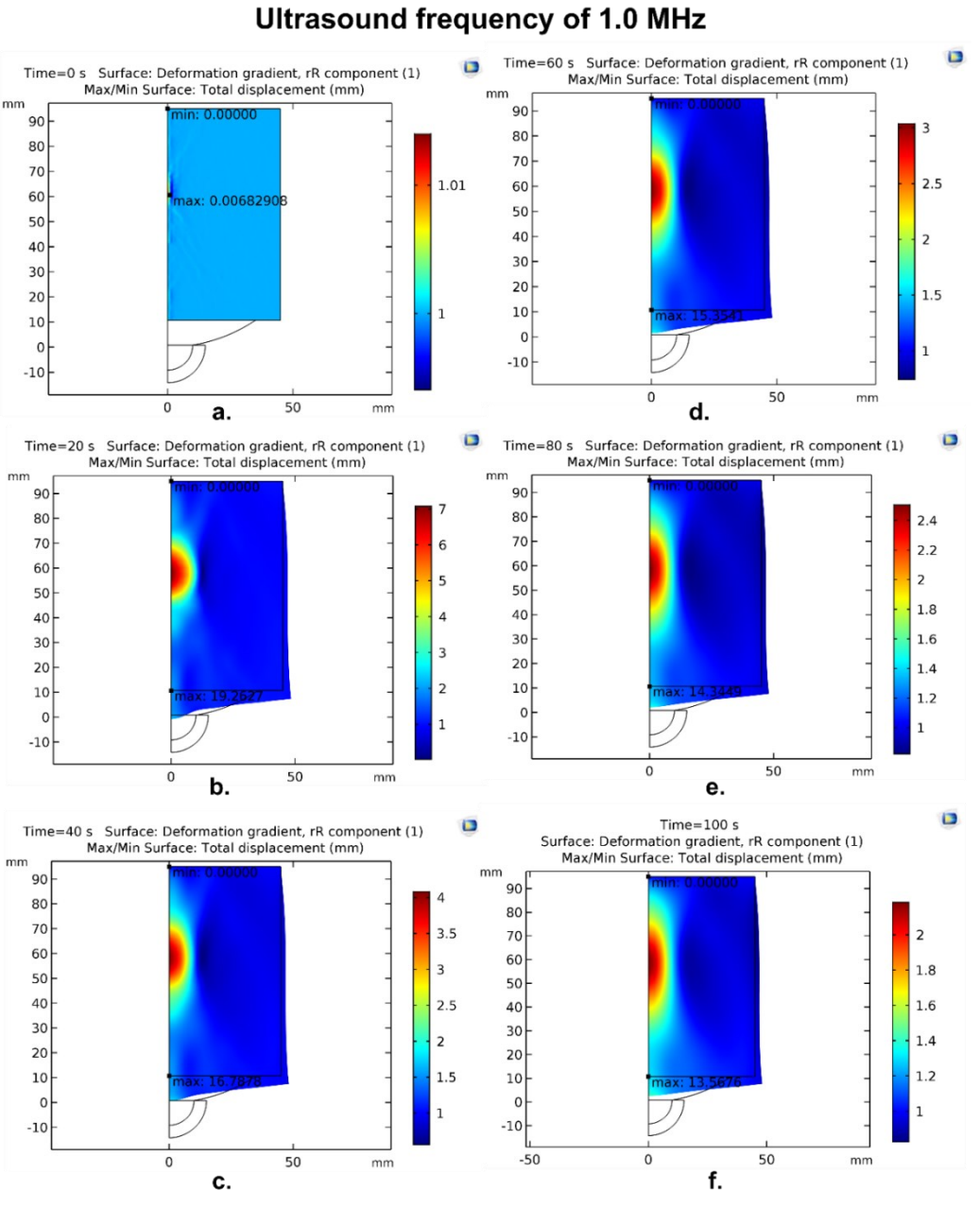

Fig. 7 The temporal evolution of total displacement in muscle tissue during ultrasound exposure at 1.0 MHz at different time intervals: (a) 0 s, (b) 20 s, (c) 40 s, (d) 60 s, (e) 80 s, and (f) 100 s.

and deeper heat distribution than the 1.5 MHz frequency, which restricted heat distribution to a narrower range (~10 arc length units). The extensive heat distribution at 1.0 MHz renders it appropriate for addressing deeper muscular tissues, including the lower back. In contrast, the 1.5 MHz frequency concentrates energy in superficial layers, rendering it optimal for muscles in regions such as the neck, shoulders, and upper back. During prolonged periods (50–100 seconds), the temperature in the impacted regions diminished as a result of heat transfer to adjacent tissues. Nonetheless, the 1.5 MHz frequency demonstrated a more rapid decrease in temperature than the 1.0 MHz frequency, indicating the swift energy absorption in the superficial tissue layers.[32]

Fig. 7 depicts the comprehensive displacement distribution in muscle tissue across time (0s, 20s, 40s, 60s, 80s, and 100s) during ultrasound therapy, with a color gradient denoting deformation magnitude and red regions signifying maximal displacement. At 0 seconds, the displacement is minimal (0.0013 mm), indicating an undisturbed equilibrium state. At 20 seconds, displacement significantly rises to 13.88 mm, reflecting the tissue's early reaction to ultrasonic wave propagation. At 40 seconds, the highest displacement is significant at 12.75 mm, indicating persistent mechanical deformation. At 60 seconds, a minor decrease to 11.96 mm indicates partial energy dissipation. This tendency persists at 80 and 100 seconds, with displacement progressively diminishing to 11.33 mm and 10.80 mm, respectively, signifying a stability phase as the tissue acclimatizes to

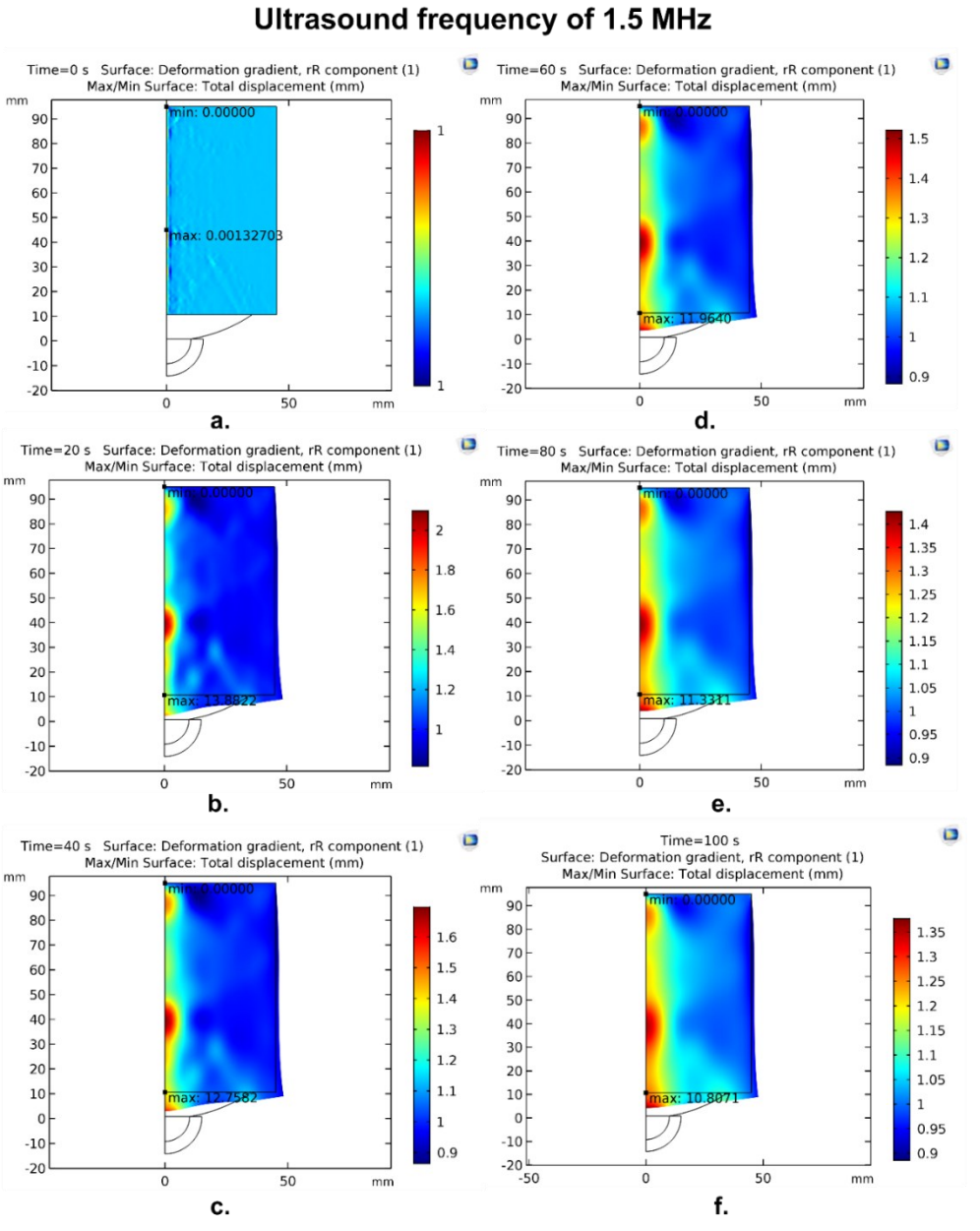

Fig. 8 The temporal evolution of total displacement in muscle tissue during ultrasound exposure at 1.5 MHz at different time intervals: (a) 0 s, (b) 20 s, (c) 40 s, (d) 60 s, (e) 80 s, and (f) 100 s.

extended ultrasonic exposure. These findings highlight the dynamic characteristics of ultrasound-induced tissue deformation and the gradual reduction of mechanical effects over time.

Fig. 8 depicts the temporal progression of total displacement in muscle tissue exposed to 1.5 MHz ultrasound for a duration of 100 seconds, demonstrating the dynamic mechanical response to wave propagation. At 0 seconds, the displacement is negligible (0.0013 mm), indicating the tissue's equilibrium state. By 20 seconds, the maximum displacement peaks at 13.38 mm, marking the onset of significant ultrasound-induced deformation. As exposure continues, displacement remains substantial, reaching 12.75 mm at 40 seconds, indicating sustained wave propagation. At 60 seconds, a minor decrease to 11.96 mm indicates the commencement of energy dissipation. This trend persists at 80 and 100 seconds, with displacement decreasing to 13.33 mm and 10.80 mm, respectively, signaling a gradual stabilizationas the tissue adapts. These findings highlight the time-dependent mechanical properties of muscle tissue subjected to therapeutic ultrasound, stressing the intricate interaction among wave-induced deformation, energy absorption, and tissue relaxation dynamics.

The mechanical displacement in tissue during ultrasonic exposure results from the pressure of propagating waves, causing viscoelastic deformation influenced by tissue characteristics like viscosity and elastic modulus. In the first phase (0–20s), displacement escalates as mechanical energy accumulates, propelled by acoustic radiation forces that produce alternating compressive and rarefactive pressures. At

40s, peak displacement signifies the optimal interaction between ultrasonic energy and tissue structure, illustrating the absorption capability of the viscoelastic medium. Beyond this juncture, energy dissipation transpires through viscous damping and the transformation of mechanical energy into heat via scattering and absorption processes. The incremental decrease in displacement in the 60s, 80s, and 100s indicates tissue adaptation by molecular reorganization, alleviating internal tension and resulting in a stabilized equilibrium state. These findings underscore the dynamic mechanical response of tissue to ultrasound and its therapeutic ramifications, including improved blood circulation, tissue regeneration, and analgesia. Prolonged exposure may cause mechanical fatigue and diminish tissue responsiveness, highlighting the necessity for optimum ultrasonic therapy duration to achieve a balance between efficacy and tissue adaptation.

Fig. 9 depicts the temporal progression of the deformation gradient (rR component) in muscle tissue subjected to ultrasound at two frequencies, 1.0 MHz (Fig. 9a) and 1.5 MHz (Fig. 9b), offering insights into the tissue's response to mechanical stress over a duration of 0s to 100s. At 1.0 MHz, the deformation gradient reaches a maximum of roughly 2.8 near the surface, then diminishing down the arc length. The most significant mechanical response is observed in the initial phase (0s–20s), followed by a reduction attributed to energy dissipation and tissue adaptation. Conversely, at 1.5 MHz, a comparable pattern is noted, but with a marginally reduced peak (~2.5), indicating a more uniformly distributed mechanical action. The elevated frequency facilitates a regulated and consistent deformation response, diminishing localized stress concentrations while preserving therapeutic effectiveness. Both frequencies exhibit a time-dependent dissipation effect, signifying tissue adaptation and diminished mechanical responsiveness with extended exposure. These findings highlight the significance of frequency optimization in ultrasound therapy, indicating that 1.0 MHz may be advantageous for deeper tissue penetration, whereas 1.5 MHz provides a more localized and controlled therapeutic effect, thereby enhancing numerical modeling for muscle pain and office syndrome treatment.

3.6 Comparative performance analysis with existing literature

The present study's significance and novelty are highlighted by contrasting the numerical modeling outcomes with previously published research on therapeutic ultrasound. The existing simulation model offers detailed, frequency-sensitive evaluations of tissue displacement and thermal profiles, a topic that has been inadequately explored in prior research. Reher *et al*.[38] performed in vitro comparisons of ultrasound devices operating at 1 MHz and 45 kHz for applications related to bone treatments. Their work exhibited variations in therapeutic penetration; however, it did not incorporate a coupled thermal-mechanical simulation framework, thereby restricting its applicability to muscle-based therapy. In contrast, our model incorporates viscoelastic deformation alongside bioheat transfer, providing a more thorough analysis. Leonard and Merrick examined intramuscular temperature variations utilizing 1.0 MHz ultrasound,[36] noting peak heating at a depth of 3–5 cm after a duration of 10 minutes. Their findings support the overall effectiveness of low-frequency ultrasound; however, the study lacked mechanical stress analysis and did not investigate frequency-dependent tissue adaptation. The model demonstrates that mechanical displacement reaches its peak at approximately 20 seconds, subsequently decreasing due to energy dissipation, which corresponds with tissue adaptation behavior. Gong *et al*.[10,11] utilized COMSOL Multiphysics to model thermal propagation in tissues.

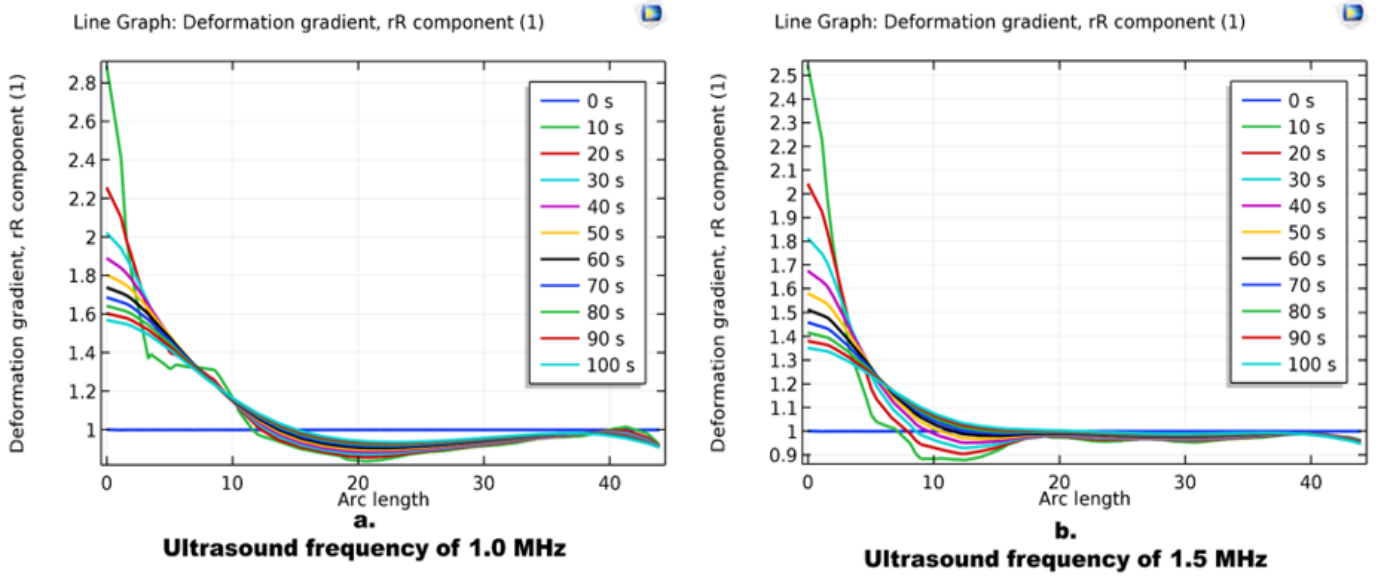

Fig. 9 Temporal evolution of the deformation gradient (rR component) in muscle tissue during ultrasound exposure at two frequencies: (a) 1.0 MHz and (b) 1.5 MHz, evaluated over time intervals from 0 to 100.

Nonetheless, their research focused mainly on heat distribution, lacking the incorporation of deformation metrics. This study demonstrates that thermal and mechanical phenomena occur concurrently, with mechanical effects occurring prior to thermal stabilization, a sequence essential for personalized treatment planning. Wood and Sehgal conducted a review on the application of low-intensity ultrasound in cancer therapy,[40] focusing mainly on biological endpoints for therapeutic optimization. This study enhances existing findings through numerical simulations of the complete therapeutic window, enabling clinicians to assess treatment efficacy prior to animal trials. Trujillo *et al.* introduced numerical advancements in modeling; however, they did not address metrics related to tissue deformation. The findings indicate that at 1.0 MHz, the displacement initially reaches approximately 13.88 mm, whereas at 1.5 MHz, the maximum displacement is lower and more uniformly distributed, contributing to a reduction in localized stress, a factor not highlighted in their report. This simulation directly addresses the existing gap by quantifying optimal exposure times and temperature thresholds (~40.09 °C at 1.0 MHz compared to ~36.3 °C at 1.5 MHz), thereby facilitating the development of standardized protocols.

This study validates prior thermal models and extends them by incorporating mechanical strain effects and frequency-based parameter tuning. This dual-modal approach improves the accuracy and safety of ultrasound therapy, establishing it as a significant computational resource for musculoskeletal disorders such as office syndrome.

Recent advances underscore the diverse applications of ultrasound beyond its biomedical heating effects. Ultrasound-Assisted Extraction of Bioactive Compounds from Sesbania javanica Flower illustrates that ultrasound significantly enhances the release of phenolic compounds, leading to improved antioxidant and antimicrobial activities.[41] This study highlights the role of ultrasound-induced acoustic cavitation and localized heating in contributing to tissue-level thermal effects, as examined in our research, as well as to improved mass transfer and cell wall disruption in plant matrices. These findings highlight the interdisciplinary influence of ultrasound, encompassing therapeutic and diagnostic biomedical applications, as well as food technology and natural product extraction. This study enhances existing research by examining spatiotemporal temperature distribution at varying frequencies (1.0 vs. 1.5 MHz), which is essential for optimizing ultrasound applications in various scientific fields.

4. Conclusion

This study employs numerical simulations in COMSOL Multiphysics software, utilizing the FEM, to investigate the impact of ultrasound waves on muscle tissue, with the aim of enhancing the effectiveness of ultrasound-based office syndrome treatment. The study optimizes frequency and treatment duration to reduce pain and inflammation. Heat from ultrasound waves reduces muscle tension, increases blood circulation. Ultrasound at 1.0 MHz can treat deeper muscles like the lower back. Neck and shoulder superficial muscles respond well to 1.5 MHz ultrasound. This therapy helps repair tissues damaged by extended sitting or poor posture. This research will help develop non-pharmacological and non-invasive treatments, reduce surgical risks, and standardize clinical applications. Moreover, the numerical simulation clearly illustrates the influence of ultrasonic waves on muscle tissue, highlighting significant changes in displacement over time. These insights can assist doctors in enhancing ultrasonic therapy parameters to maximize treatment efficacy while reducing unwanted effects. The findings corroborate the current literature, hence reinforcing the simulation model's precision and relevance in therapeutic ultrasound research. The findings facilitate the development of effective treatment strategies for office syndrome, especially for individuals experiencing prolonged sitting or repetitive strain behaviors. It provides secure and non-invasive therapeutic techniques, minimizing surgical hazards. Numerical simulations diminish the costs and duration associated with conventional experimental research. This study establishes a standardized physics-based framework for the development of ultrasound therapies for various conditions, including chronic pain in deeper muscle tissues. This research signifies a significant advancement in the development of systematic and efficient therapeutic methodologies, promoting future advancements in ultrasound-based treatments.

Acknowledgements

Thailand Science Research and Innovation Fundamental Fund fiscal year 2023 and 2024, the National Research Council of Thailand (Grant No. N42A650197) and Thammasat University Research Unit in Application of Technology and Automation Systems in Industrial for Sustainability, supported this study.

Conflict of Interest

There is no conflict of interest.

Supporting Information

Applicable.

CRediT statement

Prempreeya Montienthong: Writing – Original draft, review & editing, Methodology, Investigation, Formal analysis, Data curation, Visualization, Validation. **Phadungsak Rattanadecho:** Supervision, Conceptualization, Methodology, Resources, Project administration, Funding acquisition. **Nattapon Jaisumroum:** Funding acquisition, Writing – review & editing.

References

[1] D. O. Draper and M. D. Ricard, Rate of temperature decay in human muscle following 3 MHz ultrasound: The stretching window revealed, *Journal of Athletic Training*, 1995, 30, 304-

307.
[2] T. Watson, Ultrasound in contemporary physiotherapy practice, *Ultrasonics*, 2008, **48**, 321-329, doi: 10.1016/j.ultras.2008.02.004.
[3] D. Bhargava, P. Rattanadecho, Microwave imaging of breast cancer: simulation analysis of SAR and temperature in tumors for different age and type, *Case Studies in Thermal Engineering*, 2022, **31**, 101843, doi: 10.1016/j.csite.2022.101843.
[4] V. Mongkol, W. Preechaphonkul, P. Rattanadecho, Photo-thermo-mechanical model for laser hair removal simulation using multiphysics coupling of light transport, heat transfer, and mechanical deformation (case study), *Case Studies in Thermal Engineering*, 2023, **41**, 102562, doi: 10.1016/j.csite.2022.102562.
[5] P. Montienthong, P. Rattanadecho, Focused ultrasound ablation for the treatment of patients with localized deformed breast cancer: computer simulation, *Journal of Heat Transfer*, 2019, **141**, 101101, doi: 10.1115/1.4044393.
[6] T. Wessapan, P. Rattanadecho, Acoustic streaming effect on flow and heat transfer in porous tissue during exposure to focused ultrasound, *Case Studies in Thermal Engineering*, 2020, **21**, 100670, doi: 10.1016/j.csite.2020.100670.
[7] T. Wessapan, P. Rattanadecho, Flow and heat transfer through a porous tumor during high-intensity focused ultrasound, *International Journal of Heat and Mass Transfer*, 2023, **216**, 124501, doi: 10.1016/j.ijheatmasstransfer.2023.124501.
[8] P. Wongchadakul, P. Rattanadecho, K. Jiamjiroch, Experimental analysis of thermal transport in low-level laser therapy on skin tissue: The influence on therapeutic efficacy, pain sensation and dry skin wound, *International Journal of Thermal Sciences*, 2024, **199**, 108886, doi: 10.1016/j.ijthermalsci.2024.108886.
[9] P. Wongchadakul, P. Rattanadecho, T. Wessapan, Implementation of a thermomechanical model to simulate laser heating in shrinkage tissue (effects of wavelength, laser irradiation intensity, and irradiation beam area), *International Journal of Thermal Sciences*, 2018, **134**, 321-336, doi: 10.1016/j.ijthermalsci.2018.08.008.
[10] Z. Gong, C. Tao, X. Liu, and M. Deng, Numerical investigation on improving photoacoustic imaging contrast based on temperature difference effect in biological tissues, *Applied Acoustics*, 2023, 212, 108486, doi: 10.1016/j.apacoust.2023.109585
[11] C. Gong, B. Yang, Y. Shi, Z. Liu, and L. Wan, Factors influencing the ablative efficiency of high-intensity focused
[12] P. Bowary, B. D. Greenberg, Noninvasive focused ultrasound for neuromodulation a review, *Psychiatric Clinics of North America*, 2018, **41**, 505-514, doi: 10.1016/j.psc.2018.04.010.
[13] G. J. Landry, D. Louie, D. Giraud, A. Y. Ammi, S. Kaul, Ultrasound therapy for treatment of lower extremity intermittent claudication, *The American Journal of Surgery*, 2021, **221**, 1271-1275, doi: 10.1016/j.amjsurg.2021.02.017.
[14] J. Moreno-Moraga, T. Valero-Altés, A. M. Riquelme, M. I. Isarria-Marcosy, J. R. de la Torre, Body contouring by non-invasive transdermal focused ultrasound, *Lasers in Surgery and Medicine*, 2007, **39**, 315-323, doi: 10.1002/lsm.20478.
[15] K. Neven, B. Schmidt, A. Metzner, K. Otomo, D. Nuyens, T. De Potter, K. R. J. Chun, F. Ouyang, K. H. Kuck, Fatal end of a safety algorithm for pulmonary vein isolation with use of high-intensity focused ultrasound, *Circulation: Arrhythmia and Electrophysiology*, 2010, **3**, 260-265, doi: 10.1161/circep.109.922930.
[16] J. H. Rigby, R. M. Taggart, K. L. Stratton, G. K. Lewis Jr, D. O. Draper, Intramuscular heating characteristics of multihour low-intensity therapeutic ultrasound, *Journal of Athletic Training*, 2015, **50**, 1158-1164, doi: 10.4085/1062-6050-50.11.03.
[17] T. Wessapan, P. Rattanadecho, Thermal effects of metal implants embedded in different layers of human tissues exposed to electromagnetic fields, *Case Studies in Thermal Engineering*, 2024, **53**, 103771, doi: 10.1016/j.csite.2023.103771.
[18] Y. Wu, S. Zhu, Z. Lv, S. Kan, Q. Wu, W. Song, G. Ning, S. Feng, Effects of therapeutic ultrasound for knee osteoarthritis: a systematic review and meta-analysis, *Clinical Rehabilitation*, 2019, **33**, 1863-1875, doi: 10.1177/0269215519866494.
[19] X. Y. Zhou, X. X. Zhang, G. Y. Yu, Z. C. Zhang, F. Wang, Y. L. Yang, M. Li, X. Z. Wei, Effects of low-intensity pulsed ultrasound on knee osteoarthritis: a meta-analysis of randomized clinical trials, *BioMed Research International*, 2018, **2018**, 7469197, doi: 10.1155/2018/7469197.
[20] S. Supasin, C. Kantala, P. Intra, S. Vongpradubchai, P. Rattanadecho, Investigating the effect of pulsed electric field parameters on the quality of processed mango pickling, *Engineered Science*, 2024, **29**, 1090, doi: 10.30919/es1090.
[21] W. Klinbun, P. Rattanadecho, A computational analysis of how the design of multicompartment containers and placement angle affect heat and mass transfer during the microwave heating process, *Engineered Science*, 2023, **26**, 970, doi: 10.30919/es970.
[22], W. Preechaphonkul, P. Rattanadecho, The effects of dielectric & thermal property functions on the thermal response during the focused microwave ablation treatment in the liver cancer model: numerical investigation, *Engineered Science*, 2022, **21**, 788, doi: 10.30919/es8e788.
[23] N. Makul, G. Suaiam, New insights into the early age time dependent dielectric evolution of pozzolan modified eco efficient cement pastes within a frequency range of 200 MHz to 6500 MHz: experiments and statistical modeling experiments and statistical modeling, *Engineered Science*, 2024, **31**, 1170, doi: 10.30919/es1170.
[24] S. Supasin, C. Kantala, P. Intra, S. Vongpradubchai, P. Rattanadecho, Investigating the effect of pulsed electric field parameters on the quality of processed mango pickling, *Engineered Science*, 2024, **29**, 1090, doi: 10.30919/es1090.
[25] C. Chaki, L. De Taboada, K. M. Tse, Comparative analysis of pulsed and continuous wave modes in high-intensity laser light therapy: Implications for deep tissue treatment, *Journal of Biophotonics*, 2025, **18**, 7, doi: 10.1002/jbio.202400164.
[26] J. Dai, X. Wang, B. Zhu, L. Liang, H. C. Chang, Learning-based rapid phase-aberration correction and control for robot-assisted MRI-guided low-/high-intensity focused ultrasound treatments, *Journal of Field Robotics*, 2025, **42**, 3935-3951,

doi: 10.1002/rob.22606.
[27] H. M. M. Ten Eikelder, D. Bošnački, A. Elevelt, K. Donato, A. Di Tullio, B. J. T. Breuer, J. H. Van Wijk, E. V. M. Van Dijk, D. Modena, S. Y. Yeo, Modelling the temperature evolution of bone under high intensity focused ultrasound, *Physics in Medicine and Biology*, 2016, **61**, 1810, doi: 10.1088/0031-9155/61/4/1810.
[28] A. Paul, A. Paul, In vitro thermal assessment of vascularized tissue phantom in presence of gold nanorods during photo-thermal therapy, *Journal of Heat Transfer*, 2020, **142**, 101201, doi: 10.1115/1.4047371.
[29] D. O. Draper, J. C. Castel, D. Castel, Rate of temperature increase in human muscle during 1 MHz and 3 MHz continuous ultrasound, *The Journal of Orthopaedic and Sports Physical Therapy*, 1995, **22**, 142-150, doi: 10.2519/jospt.1995.22.4.142.
[30] V. J. Robertson, K. G. Baker, A review of therapeutic ultrasound: effectiveness studies, *Physical Therapy*, 2001, **81**, 1339-1350, doi: 10.1093/ptj/81.7.1339.
[31] F. A. Duck, *Physical Properties of Tissues: A Comprehensive Reference Book*. London, UK: Academic Press, 2013.
[32] J. G. Noble, V. Lee, F. Griffith-Noble, Therapeutic ultrasound: The effects upon cutaneous blood flow in humans, *Ultrasound in Medicine & Biology*, 2007, **33**, 279-285, doi: 10.1016/j.ultrasmedbio.2006.08.001.
[33] H. H. Pennes, Analysis of tissue and arterial blood temperatures in the resting human forearm. 1948, *Journal of Applied Physiology*, 1998, **85**, 5-34, doi: 10.1152/jappl.1998.85.1.5.
[34] M.-K. Sun, J. Shieh, C.-S. Chen, H. Chiang, C. W. Huang, and W. S. Chen, Effects of an implant on temperature distribution in tissue during ultrasound diathermy, *Ultrasonics Sonochemistry*, 2016, **32**, 44–53, doi: 10.1016/j.ultsonch.2016.02.019.
[35] P. Wongchadakul, A. K. Datta, P. Rattanadecho, Natural convection effects on heat transfer in a porous tissue in 3-D radiofrequency cardiac ablation, *International Journal of Heat and Mass Transfer*, 2023, **204**, 123832, doi: 10.1016/j.ijheatmasstransfer.2022.123832.
[36] J. Leonard, M. Merrick, C. Ingersoll, M. Cordova, A comparison of intramuscular temperatures during 10-minute 1.0-MHz ultrasound treatments at different intensities, *Journal of Sport Rehabilitation*, 2004, **13**, 244–254, doi: 10.1123/jsr.13.3.244.
[37] P. O. Burr, T. J. Demchak, M. L. Cordova, C. D. Ingersoll, M. B. Stone, Effects of altering intensity during 1-MHz ultrasound treatment on increasing triceps surae temperature, *Journal of Sport Rehabilitation*, 2004, **13**, 275-286, doi: 10.1123/jsr.13.4.275.
[38] P. Reher, N. Doan, B. Bradnock, S. Meghji, M. Harris, Therapeutic ultrasound for osteoradionecrosis: an *in vitro* comparison between 1 MHz and 45 kHz machines, *European Journal of Cancer*, 1998, **34**, 1962-1968, doi: 10.1016/s0959-8049(98)00238-x.
[39] V. Robertson, A. Ward, J. Low, A. Reed, *Electrotherapy Explained: Principles and Practice*, London, U.K: Elsevier Health Sciences, 2006, ISBN: 978-0-7506-8896-4.
[40] A. K. W. Wood, C. M. Sehgal, A review of low-intensity ultrasound for cancer therapy, *Ultrasound in Medicine & Biology*, 2015, **41**, 905-928, doi: 10.1016/j.ultrasmedbio.2014.11.019.
[41] S. Chheng, M. Fikry, S. Jafari, S. K. Mehta, D. K. Mishra, K. Assatarakul, Ultrasound-assisted extraction of bioactive compounds from sesbania javanica flower: phenolic composition, antioxidant, and antimicrobial applications, *ES Food & Agroforestry*, 2025, **19**, 1434, doi: 10.30919/faf1434.